

## Article

# Modeling of the Suspended Solid Removal of a Granular Media Layer in an Upflow Stormwater Runoff Filtration System

Yuhoon Hwang <sup>1</sup>, Younggyo Seo <sup>1</sup>, Seokoh Ko <sup>2,\*</sup> and Dogun Kim <sup>3,\*</sup>

<sup>1</sup> Department of Environmental Engineering, Seoul National University of Science and Technology, 232 Gongreung-ro, Nowon-gu, Seoul 01811, Korea; yhhwang@seoultech.ac.kr (Y.H.); syg9996@seoultech.ac.kr (Y.S.)

<sup>2</sup> Department of Civil Engineering, Kyung Hee University, 1732, Deogyong-daero, Giheung-gu, Yongin-si 17104, Korea

<sup>3</sup> Department of Environmental Engineering, Sunchon National University, 255 Jungang-ro, Suncheon 57922, Korea

\* Correspondence: soko@khu.ac.kr (S.K.); dgkim@scnu.ac.kr (D.K.); Tel.: +82-31-210-2999 (S.K.); +82-61-750-3827 (D.K.)

**Abstract:** Upflow granular media filtration devices are widely used for stormwater runoff treatment. However, the system performance is not well characterized due to the irregular removal of suspended solid (SS) in the pretreatment (sedimentation) chamber and, hence, its irregular input to the media layer. In this regard, the performance of the granular media layer of an upflow filtration system is investigated herein by the use of various models. Due to the significant variation in the SS concentration of the influent and effluent to and from the media layer, the deep bed filtration model, the  $k-C^*$  model, and the porous media capture model provide limited descriptions of the system performance. By contrast, the performance is well described using the kinetic model, the modified  $k-C^*$  model using a specific deposit, and the modified porous media capture model using a specific deposit. The parameters of the latter models are shown to be in good correlation with the filtration velocity, SS removal, and specific deposit. The results suggest that modeling using a specific SS deposit can provide an accurate description of the granular media layer performance under a highly variable influent SS concentration.

**Keywords:** model; non-point source pollution; specific solid deposit; stormwater runoff; upflow granular media filtration



**Citation:** Hwang, Y.; Seo, Y.; Ko, S.; Kim, D. Modeling of the Suspended Solid Removal of a Granular Media Layer in an Upflow Stormwater Runoff Filtration System. *Appl. Sci.* **2021**, *11*, 6202. <https://doi.org/10.3390/app11136202>

Academic Editor: Faisal I. Hai

Received: 12 June 2021

Accepted: 2 July 2021

Published: 4 July 2021

**Publisher's Note:** MDPI stays neutral with regard to jurisdictional claims in published maps and institutional affiliations.



**Copyright:** © 2021 by the authors. Licensee MDPI, Basel, Switzerland. This article is an open access article distributed under the terms and conditions of the Creative Commons Attribution (CC BY) license (<https://creativecommons.org/licenses/by/4.0/>).

## 1. Introduction

It has been shown that the pollutants from non-point, or diffuse, sources contribute significantly to the pollutant load in the water system, with up to 37.6% of rivers, streams, lakes, reservoirs, ponds, bays, estuaries, and coastal shorelines having their water quality adversely affected by such pollutants [1]. In particular, for the Danjiangkou reservoir, China, the non-point source contributions to the chemical oxygen demand (COD<sub>Mn</sub>) and total phosphorus (TP) load were 68.4% and 82.9%, respectively [2]. In the Republic of Korea, the emission of COD and TP from non-point sources comprised 67.6% and 72.1% (i.e., 700 and 53 tons/day), respectively, of the total load to the water system in 2018, and was predicted to be increased by 2025 [3].

The control of pollutants in stormwater runoff is of prime importance for controlling the influx of non-point source pollutants to nearby water systems, particularly in urban areas. The pollutants of natural and/or anthropogenic origins in the air and on the surface are carried by stormwater runoff and deposited in lakes, rivers, wetlands, coastal waters, and groundwater [1]. The pollutants in stormwater runoff are not limited to particulates (i.e., suspended solids (SS)), but include both dissolved and particulate forms of organic matter [4–6], heavy metals [7,8], and phosphorus [9]. Therefore, stormwater treatment

technologies such as filtration, infiltration, and constructed wetlands have been developed and applied for the reduction of non-point source pollution.

The use of granular media such as sand [10], gravel [11], and perlite [12] is a widely adopted runoff treatment process known to be most suitable in urbanized areas [10], with high removal efficiencies of SS, phosphorus, and heavy metals via several mechanisms including filtration and adsorption [13]. Granular filtration media are most frequently recommended due to their porosity, simple structure, easy operation, low price, chemical stability, and easy coating with metal (Fe or Mn) oxides/hydroxides for additional functions such as heavy-metal adsorption [14]. Various granular media have been reported, including recycled glass, foamed polymers, potting soil, coconut fiber, compost, water sludge, pumice/woodchip mixtures, and fibrous plastics [15–18].

Although granular media filtration is an excellent alternative for the treatment of stormwater runoff, it must be more elaborated for the description of the system performance. The hydraulics of the system could well be described using several models, including a power model [16,19,20]. However, the evaluation and description of the SS removal of the systems remain a great challenge. This is primarily due to the high variation in the flow rate and quality of the influent (i.e., the stormwater runoff) [19]. The size of the SS is highly heterogeneous, the concentration of the SS fluctuates significantly, and the flow rate varies greatly, even during a single rainfall event [19,21–23]. These variations can lead to phenomena that are not generally encountered in the granular media filtration systems used in water and wastewater treatment plants, e.g., migration, detachment, and re-dispersion of the trapped SS [17,21–24]. Moreover, the existence of a pretreatment chamber would induce more variation in the SS concentration in the influent of filtration chambers. A pretreatment chamber is generally a sedimentation chamber with a short retention time [25,26] and is usually installed in stormwater runoff filtration facilities to reduce the SS load on the media layer in the filtration chamber [25,26]. However, there is a variation in the SS concentration of the effluent from the sedimentation chamber; therefore, the influent of the filtration chamber is more severe due to the irregular and high fluctuation in the SS removal efficiency and to the scouring of the deposited SS [25].

Therefore, in the present study, the SS removal of an upflow granular media filtration system is analyzed using several models to identify appropriate descriptions of stormwater runoff filtration systems. The SS removal is selected for investigation because it can provide an indication of the removal of other pollutants in runoff filtration devices [27,28]. Indeed, several previous studies have reported that the runoff SS is the most important carrier and sink for other pollutants, including organic matter [4–6], heavy metals [7,8], and phosphorus [9].

## 2. Materials and Methods

### 2.1. Laboratory Scale Experiment

The instruments and experimental procedures are described in detail herein to supplement those briefly introduced in previous work [20]. Fixed bed filtration experiments were performed using a laboratory-scale filtration unit with a 900 mm deep sedimentation chamber and an 800 mm deep media chamber with a  $100 \times 100 \text{ mm}^2$  base and a media depth of 600 mm. The granular media in this study were provided by C & C Inc. (Siheung, Korea) and were prepared from shale via grinding, sintering, expanding, and molding into granular shapes. The average size, porosity, specific gravity, and water permeability were 2.92 mm, 60.7%, 1.55, and 0.14 cm/s, respectively. Schematic diagrams and pictures of the laboratory scale instruments and the granular media are provided in Figure 1.

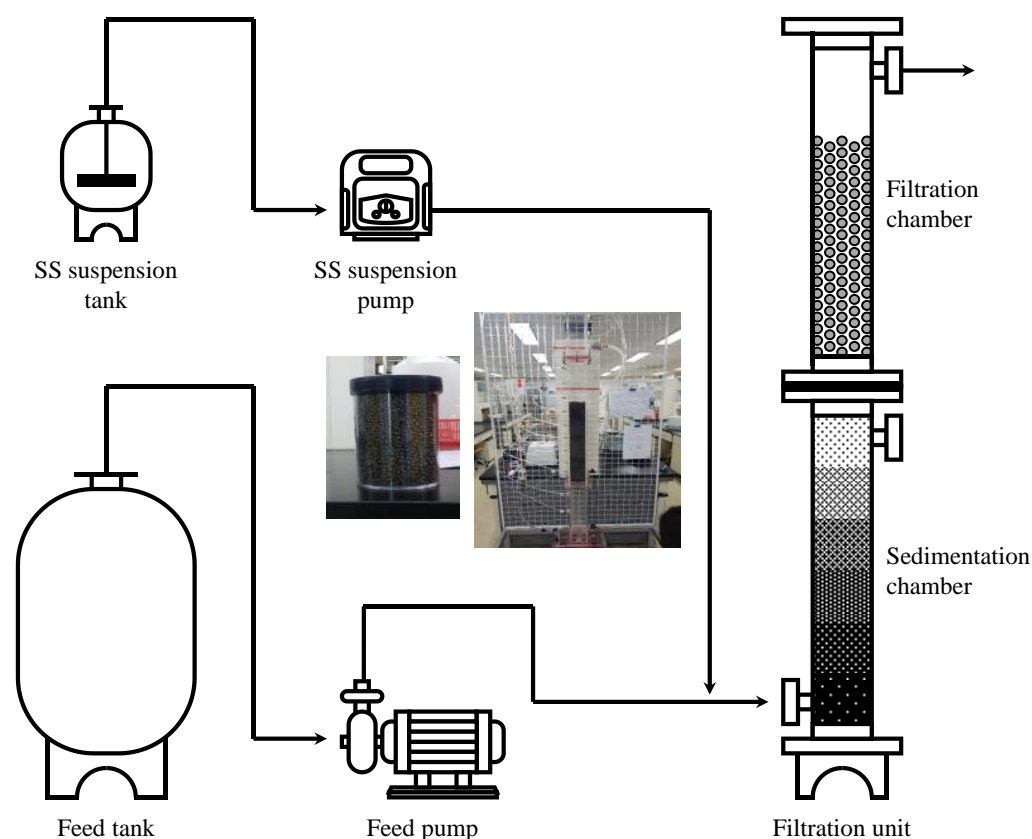


**Figure 1.** A schematic diagram of the laboratory-scale filtration system with inset photographic images of the granular media (left) and filtration chamber (right).

The road deposited sediment (RDS) on local highways was collected by road sweepers and used as SS in the present study to simulate the actual conditions experienced by stormwater runoff filtration devices. The RDS was provided by the Korea Expressway Corporation and was dried at 105 °C overnight. The fraction passed through the #60 sieve was used to match the size distribution of the SS in stormwater runoff. The average particle size was 125.6  $\mu\text{m}$ , the median size was 122.1, and the 10%, 60%, and 90% fines ( $d_{10}$ ,  $d_{60}$ , and  $d_{90}$ ) were 13.2, 122.1, and 246.2  $\mu\text{m}$ , respectively [20]. This is consistent with previous studies showing that 96.2% of stormwater runoff particles were <200  $\mu\text{m}$  in size [29], and 90% were <250  $\mu\text{m}$  [30]. Similarly, in the Republic of Korea, the  $d_{10}$ ,  $d_{60}$ , and  $d_{90}$  of the SS in stormwater runoff samples from the 39 highway were 4.2, 57.6, and 276.5  $\mu\text{m}$ , respectively [31], while those from residential and industrial areas were 0.87–5.78, 4.11–61.37, and 8.02–166.86  $\mu\text{m}$ , respectively [32], and those from a residential area were 9.82, 38.99, and 159.61  $\mu\text{m}$ , respectively [33].

The SS-free tap water and 10,000 mg/L aqueous suspensions of SS were introduced simultaneously to the sedimentation chamber so that the SS concentration of the influent was  $168.4 \pm 4.4$  mg/L. The influent was pumped upward through the sedimentation chamber and then the media chamber. Filtration velocities of 20, 30, and 40 m/h were used, giving influent flow rates of 0.2, 0.3, and 0.4  $\text{m}^3/\text{h}$ . The effluents of both chambers were collected periodically during the 300 min of operation, and the SS concentration was measured using standard methods [34]. The influent SS concentration, filtration velocity, and operation period were determined considering the protocols for the evaluation of the performance of stormwater filtration devices of the Korea Ministry of Environment [35], the New Jersey Department of Environmental Protection [36], British Water [29], and Auckland Council [30].

## 2.2. Modeling

### 2.2.1. The Kinetic Model

The kinetic model describes the attachment of SS to, and its detachment from, a filter medium in terms of the specific SS deposit per unit volume of the medium ( $\sigma$ , kg/m<sup>3</sup>) [37], as given by Equation (1):

$$\frac{\partial \sigma}{\partial t} = k_a u C_0 (\sigma_m - \sigma) - k_d \sigma \quad (1)$$

where  $\sigma$  is the specific SS deposit (kg/m<sup>3</sup>) at time  $t$  (h),  $\sigma_m$  is the maximum specific SS deposit (kg/m<sup>3</sup>),  $C_0$  is the SS concentration of the influent (kg/m<sup>3</sup>),  $u$  is the filtration velocity (m/h),  $k_a$  is the attachment constant (h<sup>-1</sup>), and  $k_d$  is the detachment constant (h<sup>-1</sup>). It is assumed that the local fluid velocity and shear stress increase due to the decrease in pore space when  $\sigma$  reaches a critical level. The elevated fluid velocity and shear stress induce the breakage of deposited SS aggregates and, hence, the discharge of the solids [38]. Consequently, the amount of SS in the effluent is increased, and the overall SS deposit, i.e.,  $\sigma$ , is decreased.

### 2.2.2. The Deep Bed Filtration Model

The deep bed filtration model is based on the general mass balance of SS for one-dimensional transport under a steady state. The transport in the z-direction can be written as in Equation (2):

$$\frac{\partial \sigma}{\partial t} + \frac{\partial \varepsilon C}{\partial t} + \frac{\partial u C}{\partial z} - \frac{\partial}{\partial z} \left( D \frac{\partial C}{\partial z} \right) = 0 \quad (2)$$

where  $\varepsilon$  and  $D$  are the porosity of the media and the dispersion coefficient (m<sup>2</sup>/h), respectively. When the SS deposit ( $\sigma$ ) is much higher than the temporary variation in the pore SS concentration, and when the dispersion of SS in the media layer is negligible, Equation (2) can be replaced by Equation (3) [37]:

$$u \frac{\partial C}{\partial z} = - \frac{\partial \sigma}{\partial t} \quad (3)$$

Then, one of the most widely adapted approaches for the evaluation of migration, retention, and detachment, namely, the Iwasaki Equation (Equation (4) below), is combined with Equation (3) to give Equation (5) [39]:

$$\frac{\partial C}{\partial z} = -\lambda C \quad (4)$$

$$\frac{\partial \sigma}{\partial t} = u \lambda C \quad (5)$$

where  $\lambda$  is the filter coefficient (m<sup>-1</sup>) at time  $t$  or at bed depth  $z$ , and represents the probability of SS being present in the porous media, and is the inverse of the maximum average penetration depth of SS in the media layer. Thus,  $\lambda$  increases with increasing SS retention or deposition (i.e., increasing  $\sigma$ ) [40,41]. The  $\lambda$  value is the dominant parameter in the filtration of solids, i.e., in the transport of solids through, and their deposition in, a porous medium, and is related to the pore space. Therefore,  $\lambda$  is related to the SS deposit according to Equation (6) [42]:

$$\lambda = \lambda_0 \left( 1 - \frac{\sigma}{\sigma_m} \right)^a \quad (6)$$

where  $\lambda_0$  is the  $\lambda$  value of the clean filter medium and is obtained using the initial SS concentrations of the influent and effluent.

### 2.2.3. The $k$ - $C^*$ Model

The  $k$ - $C^*$  model describes the overall performance of an individual layer in terms of the pseudo-first-order kinetics under steady-state conditions, as in Equation (7) [11,43]:

$$\frac{C - C^*}{C_0 - C^*} = e^{-k_C H/u} \quad (7)$$

where  $C$  is the effluent SS concentration (mg/L) at time  $t$ ,  $C_0$  is the influent SS concentration (mg/L),  $C^*$  is the background SS concentration (mg/L),  $u$  is the hydraulic loading (m/h),  $H$  is the depth of an individual layer (m), and  $k_C$  is the rate constant ( $\text{h}^{-1}$ ). Equation (7) can be expressed as Equations (8) and (9) by substituting  $C^*$  for  $A_C$ :

$$\frac{C}{C_0} = A_C e^{-k_C H/u} \quad (8)$$

$$\ln\left(\frac{C}{C_0}\right) = \ln(A_C) - k_C \frac{H}{u} \quad (9)$$

where  $A_C$  is a constant. The effects of various SS removal mechanisms (i.e., diffusion, straining, adhesion, interception, and sedimentation) are collectively represented by  $k_C$  and  $A_C$ , whose values are influenced by the pollutant concentration and hydraulic conditions [44]. Previously, the time-courses of SS removal have been predicted using the  $k$ - $C^*$  model for wastewater filtration and stormwater treatment systems such as infiltration systems, swales, constructed wetlands, and gravel filters [11,44,45]. In the present study, however, Equation (9) is modified by considering the SS load and the specific deposit (i.e.,  $\sigma$ , as presented in Equations (10) and (11) below) because it is thought that the SS concentration might not represent the performance of the system due to the irregular inlet and outlet SS concentrations induced by the sedimentation chamber:

$$\ln\left(\frac{L}{L_0}\right) = \ln(A_L) - k_L \frac{H}{u} \quad (10)$$

$$\ln(\sigma) = \ln(A_\sigma) - k_\sigma \frac{H}{u} \quad (11)$$

where  $L$ ,  $L_0$ , and  $\sigma$  ( $\text{kg}/\text{m}^3$ ) are the outlet SS load, inlet SS load, and specific deposit at time  $t$ , respectively;  $A_L$  and  $A_\sigma$  are the constants corresponding to the SS loads and the specific deposit, respectively; and  $k_L$  and  $k_\sigma$ , are the rate constants corresponding to the SS loads and specific deposit, respectively.

### 2.2.4. The Steady-State Porous Media Capture Equation

The porous media capture equation under steady-state conditions describes the decrease in SS concentration in the effluent with increasing porosity and/or depth of the media, as in Equation (12) [46]:

$$\ln\left(\frac{C}{C_0}\right) = -\frac{3}{2} \frac{(1-\varepsilon)}{D_c} \alpha_s \eta H \quad (12)$$

where  $\alpha_s$ ,  $D_c$ , and  $\eta$  are the sticking coefficient, the collector particle diameter, and the single collector collision efficiency, respectively. These three parameters can be combined into a single coefficient,  $X_C$ , that increases with decreasing permittivity of SS (and, hence, with decreasing SS concentration in the effluent), as in Equation (13) [16]:

$$\ln\left(\frac{C}{C_0}\right) = -\frac{3}{2} X_C (1-\varepsilon) H \quad (13)$$

Moreover,  $C/C_0$  in Equation (13) can be substituted for either  $L/L_0$  or  $\sigma$  in Equations (10) and (11), respectively, and the coefficient  $X_C$  can be replaced by  $X_L$  and  $X_\sigma$  to represent the

$X_C$  according to the cumulative inlet SS load or the cumulative reduced SS load, respectively, as in Equations (14) and (15):

$$\ln\left(\frac{L}{L_0}\right) = -\frac{3}{2}X_L(1-\varepsilon)H \quad (14)$$

$$\ln(\sigma) = -\frac{3}{2}X_\sigma(1-\varepsilon)H \quad (15)$$

### 3. Results and Discussion

#### 3.1. SS Removal and Head Loss

The measured SS concentrations at the influent were  $165.8 \pm 2.8$ ,  $171.6 \pm 5.1$ , and  $161.8 \pm 4.6$  mg/L; those of the effluent from the sedimentation chamber (and, hence, the influent to the filtration chamber) were  $38.0 \pm 4.0$ ,  $43.9 \pm 5.8$ , and  $45.8 \pm 6.0$  mg/L; and those of the effluent from the filtration chamber were  $2.3 \pm 0.3$ ,  $2.8 \pm 1.6$ , and  $5.1 \pm 2.6$  mg/L; for filtration velocities of 20, 30, 40 m/h, respectively, as reported previously [20]. This indicates that the SS removal in both the sedimentation chamber and filtration chamber was excellent. However, the results in Figure 2 indicate that the SS removal in each chamber varied widely with the variation in filtration velocity. Thus, the  $C/C_0$  ratio of the sedimentation chamber is  $0.185 \pm 0.057$ ,  $0.204 \pm 0.041$ , and  $0.206 \pm 0.019$ , while that of the filtration chamber is  $0.141 \pm 0.068$ ,  $0.126 \pm 0.070$ , and  $0.113 \pm 0.033$ , for filtration velocities of 20, 30, and 40 m/h, respectively. Meanwhile, the relative standard deviation of the  $C/C_0$  ratio for the sedimentation chamber is 0.310, 0.201, 0.092, while that of the filtration chamber is 0.484, 0.555, and 0.297, at 20, 30, and 40 m/h, respectively. The more significant fluctuation of the  $C/C_0$  ratio in the filtration chamber relative to that in the sedimentation chamber can be attributed to the variation in the SS removal in the latter. Moreover, the  $C/C_0$  ratio at each operation time was not correlated with the filtration velocity at either the sedimentation chamber or the filtration chamber. This might be due to the irregular re-dispersion and breakage of the deposited SS [37].

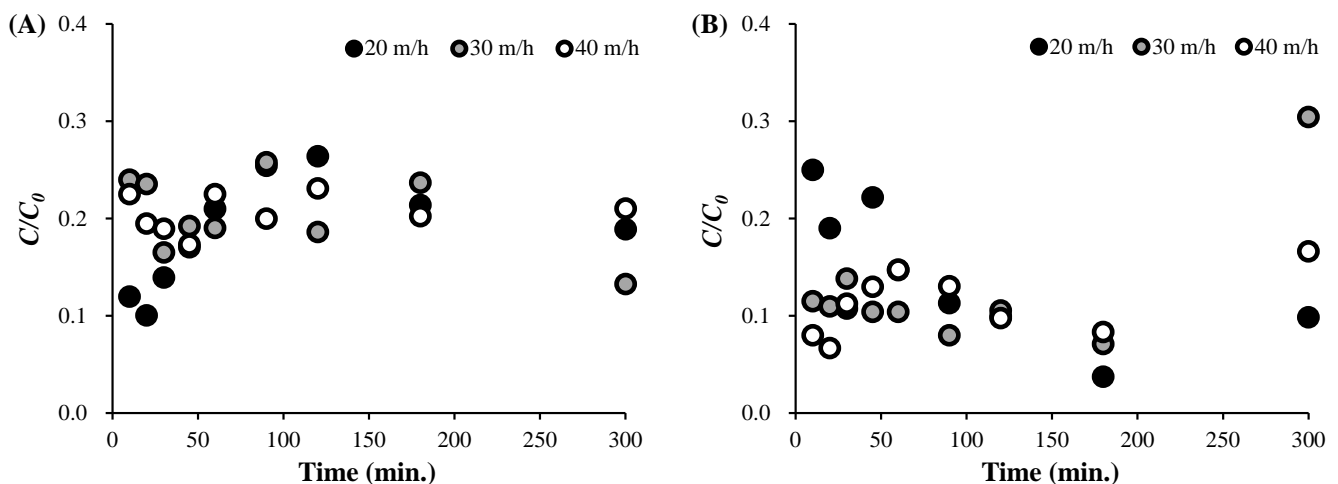


**Figure 2.** The time evolution of SS concentration in the outlets of (A) the sedimentation chamber and (B) the filtration chamber.

The measured total head loss of the clean filtration chamber (i.e., at time  $t = 0$ ) was 3.0, 4.2, and 5.6 cm, and gradually increased to maximum values of 5.3, 6.5, and 7.9 cm at  $t = 300$  min for filtration velocities of 20, 30, and 40 m/h, respectively, as reported in previous work [20]. This indicates that, although the re-dispersion and breakage of the deposited SS are expected to increase with increasing filtration velocity, a higher inlet SS load results in a higher head loss.

### 3.2. Modeling Study

#### 3.2.1. The Kinetic Model

The results of the kinetic model in Figure 3 revealed an increase in  $k_a$  and  $k_d$ , along with a decrease in  $\sigma_m$ , with increasing filtration velocity. Moreover, a good fit to the measured results was obtained for each filtration velocity, with a correlation coefficient ( $r^2$ ) of 0.98–0.99, thus suggesting that the kinetic model is useful for describing the overall performance of the system. In detail, the  $k_a$  values are seen to be  $3.16 \times 10^{-5}$ ,  $4.09 \times 10^{-5}$ , and  $7.93 \times 10^{-5} \text{ h}^{-1}$ , with corresponding  $k_d$  values of  $0.07 \times 10^{-5}$ ,  $6.03 \times 10^{-5}$ , and  $29.18 \times 10^{-5} \text{ h}^{-1}$ , and  $\sigma_{max}$  values of 901.20, 428.95, and  $306.81 \text{ kg/m}^3$ , at filtration velocities of 20, 30, and 40 m/h, respectively. The decrease in  $\sigma_m$  is attributed to an increased probability of detachment of the accumulated SS from the media with an increasing amount of accumulated SS and with increasing filtration velocity, the latter leading to higher shear stress and hydraulic gradient [37]. This conclusion is supported by the significantly greater increase in  $k_d$  relative to  $k_a$ , with increasing filtration velocity.

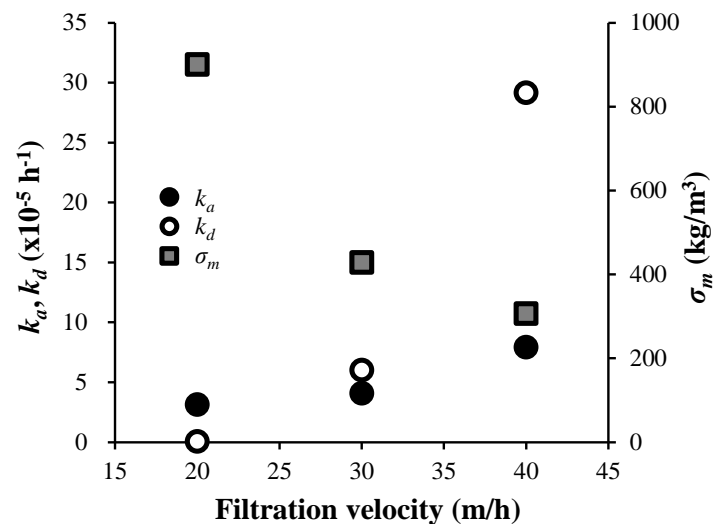


**Figure 3.** The variation in the kinetic model parameters with varying filtration velocity.

Meanwhile, the values of  $k_a$  and  $k_d$  were 1.423–3.983 and  $2.88 \text{ h}^{-1}$ , respectively, for the fibrous media with the fiber diameters of 1–26  $\mu\text{m}$  and with the porosity of 0.67–0.85 when the SS of 5  $\mu\text{m}$  was introduced [37]. This indicates that the SS accumulated on the medium in this study was more subjected to detachment, probably due to higher filtration velocity.

#### 3.2.2. The Deep Bed Filtration Model

For the deep bed filtration model, the time evolution of the parameter  $\lambda$  with varying filtration velocity is indicated in Figure 4A. Here, similar  $\lambda_0$  values of 0.536, 0.590, and  $0.575 \text{ m}^{-1}$  were obtained for filtration velocities of 20, 30, and 40 m/h, respectively. This demonstrates that  $\lambda_0$  is independent of the filtration velocity and SS concentration, in agreement with the results of a previous study [39]. Moreover, the  $\lambda$  values obtained in the present study are seen to vary in the ranges of 1.031–1.525, 1.088–1.510, and  $1.001–1.313 \text{ m}^{-1}$  at filtration velocities of 20, 30, and 40 m/h, respectively, which is also in agreement with previously reported ranges of  $0.8–269.24 \text{ m}^{-1}$  (for 0.24–0.36 mm Ottawa sand) [40] and  $140–191 \text{ m}^{-1}$  (for 0.227 mm sand) [47]. However, the results in Figure 4B indicate that the correlation between the  $\lambda$  and  $\sigma$  parameters that was proposed in Equation (6) is absent. This is attributed to the variation in the SS concentration of the effluent due to the significant heterogeneity in the amount of influent SS. The  $\lambda$  value is influenced by time as well as pore space; hence,  $\lambda$  varies with variations in the operation time, bed depth, and pore structure of the media layers [48].

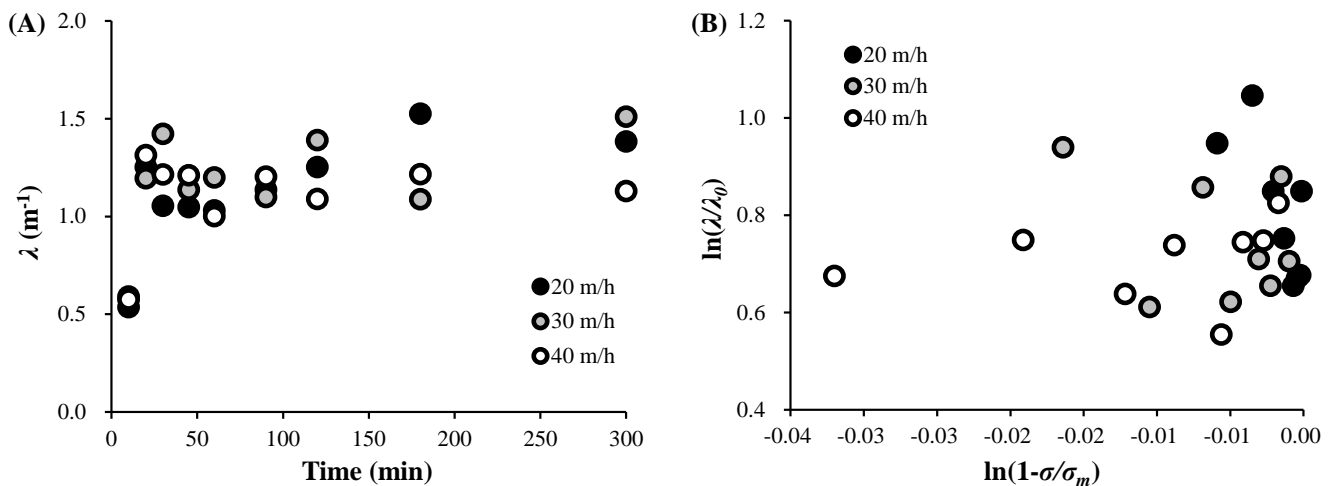


**Figure 4.** The deep bed filtration model: (A) the time evolution of  $\lambda$ ; (B) the correlations between  $\lambda$  and  $\sigma$ .

### 3.2.3. The $k$ - $C^*$ Model

For the  $k$ - $C^*$  model, the results in Figure 5A,B indicate a correlation between  $\ln(C/C_0)$  and  $H/u$  only during the initial 10–20 min of operation, and the obtained  $k_C$  values were negative. Moreover, no significant correlation was observed for the period of 30–300 min, regardless of filtration velocity. These results can be anticipated by the examination of Figure 2B above, which indicates that the SS removal is independent of both the operation time and the filtration velocity. Similarly, the results in Figure 5C,D indicate a correlation between  $\ln(L/L_0)$  and  $H/u$  only during the initial 10–60 min, with negative  $k_L$  values. The negative filtration rate constants indicate that the  $k$ - $C^*$  model, which is based on pseudo first-order SS removal, cannot accurately describe the system used in the present study. Some previous studies have reported that the  $k$ - $C^*$  model cannot be applied to the removal of SS from stormwater by filtration over the lifetime of the system because the parameters, i.e.,  $k_C$ ,  $k_L$ ,  $A_C$ , or  $A_L$ , fluctuate with SS concentration and hydraulics [45].

Nevertheless, the results in Figure 5E indicate a good correlation between  $\ln(\sigma)$  and  $H/u$  throughout the period of operation. Moreover, the results in Figure 5F indicate a gradual increase in the calculated  $k_\sigma$  and  $A_\sigma$  values during operation, thus indicating that the SS removal is enhanced with increasing  $\sigma$  and decreasing porosity. The increase in  $k_\sigma$  is consistent with the limited variation in  $C/C_0$  with filtration velocity and increasing operation period (Figure 2B). Moreover, the increase in  $A_\sigma$  is in accord with the decrease in  $\sigma_m$  with increasing filtration velocity (Figure 3). Hence, although no relationship between the parameters and the filtration conditions (e.g., SS concentration, SS characteristics, and hydraulic condition) is considered in the  $k$ - $C^*$  model [49], a modified version of this model that considers a specific deposit might successfully describe the performance of the system used in the present study. Meanwhile, the values of  $k_\sigma$  were significantly higher than the  $k_\sigma$  obtained in a wetland in Texas, USA, i.e., 0.228–6.849  $\text{h}^{-1}$  [44], indicating a faster SS removal by the media in his study.

On the other hand, it should be noted that the good correlation between the filtration velocity ( $L/u$ ) and  $\ln(X_\sigma)$  does not mean that this model describes the time variation of the influent SS concentration. The concentration of the pollutants of the influent of a stormwater treatment system generally varies with time, i.e., first, middle, and final flush, where the load of the pollutants is concentrated during the prophase, metaphase, and anaphase, respectively [50]. Therefore, a more advanced model must be developed to a better description of the SS removal in a stormwater filtration device.

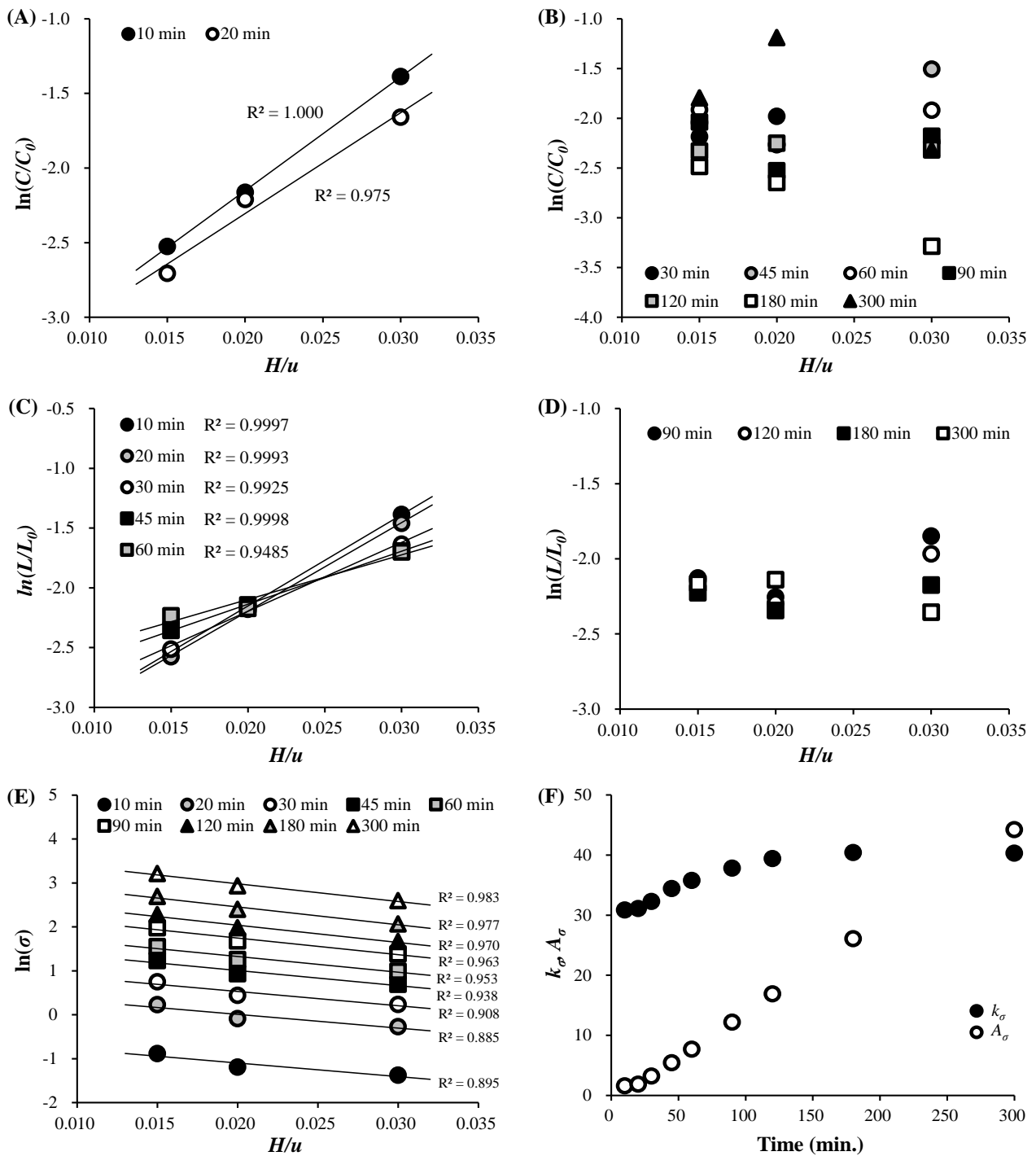


**Figure 5.** The  $k$ - $C^*$  model: (A,B) the correlation between  $\ln(C/C_0)$  and  $H/u$  during system operation times of (A) 10–20 min and (B) 30–300 min; (C,D) the correlation between  $\ln(L/L_0)$  and  $H/u$  during system operation times of (C) 10–60 min and (D) 90–300 min; (E) the correlation between  $\ln(\sigma)$  and  $H/u$ ; (F) the time evolution of  $k_\sigma$  and  $A_\sigma$ .

### 3.2.4. Steady-State, Porous Media Capture Model

The results presented in Figure 6A for the steady-state porous media capture model based on SS concentration indicate wild fluctuations in the coefficient  $X_C$  within the ranges of 3.92–9.29, 3.36–7.48, and 5.07–7.65  $m^{-1}$  at filtration rates of 20, 30, and 40 m/h, respectively. This result indicates that the steady-state porous media capture model based on SS concentration cannot be used to describe the performance of the media layer. However, the values of  $X_C$  in Figure 6A were higher than those reported in previous works. The  $X_C$  of

geosynthetic filters was in a range of  $917\text{--}1553\text{ mm}^{-1}$  [16], and that of geotextile filters was in a range of  $396\text{--}1793\text{ mm}^{-1}$  [51], indicating a higher SS capture efficiency of the media in this study.

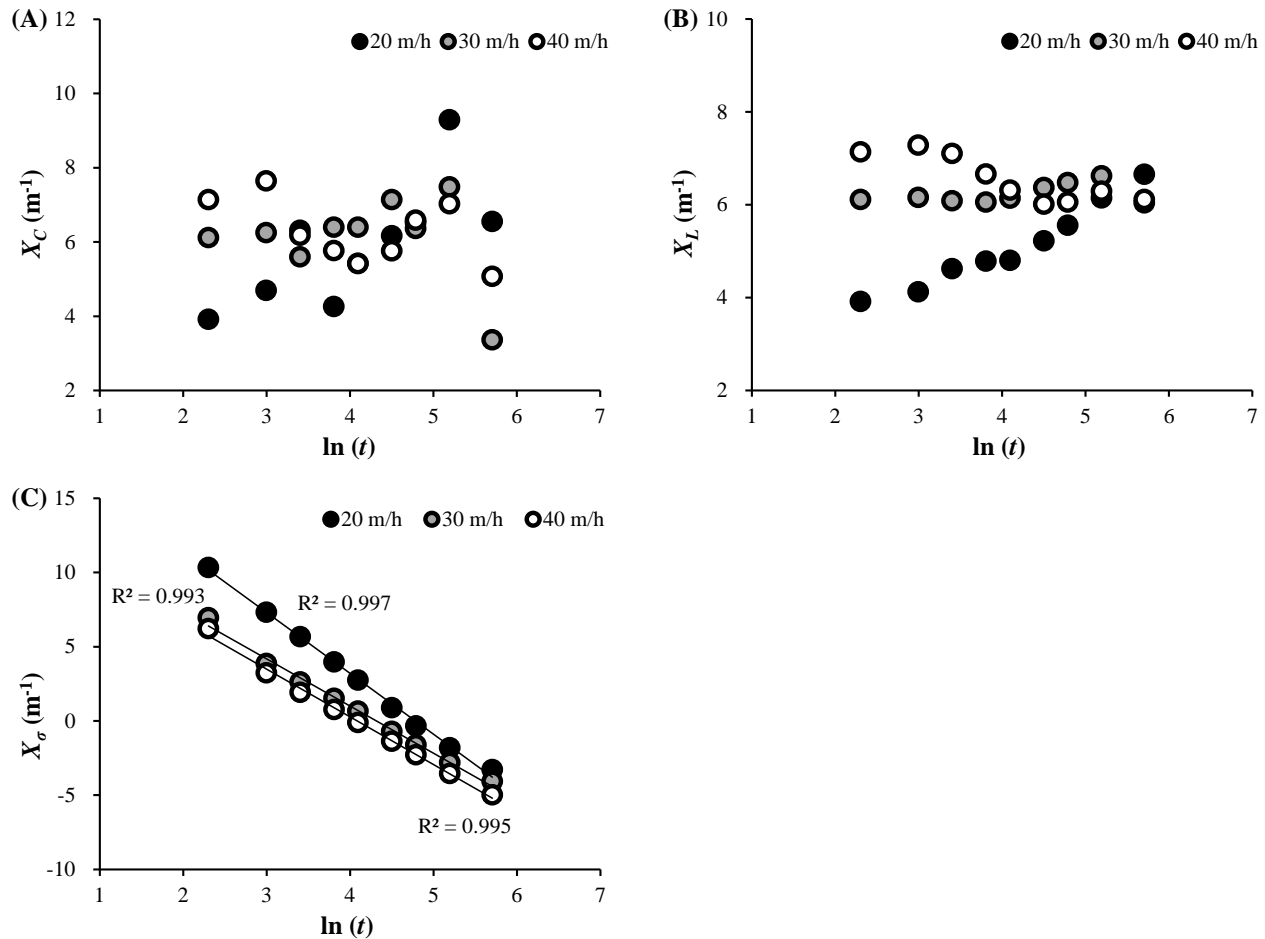


**Figure 6.** The time and filtration-velocity variations in the filtration coefficients of the media layer based on: (A) SS concentration, (B) SS load reduction, and (C) specific SS deposit.

By contrast, the results of the model based on varying SS inlet load (Figure 6B) reveals a clear correlation with the coefficient  $X_L$ . Thus: (i) the  $X_L$  value is seen to increase from  $3.92$  to  $6.66\text{ m}^{-1}$  under a low filtration velocity ( $20\text{ m/h}$ ); (ii) at the moderate filtration velocity of  $30\text{ m/h}$ , the  $X_L$  remains steady within the range of  $6.06\text{--}6.16\text{ m}^{-1}$  during the initial  $10\text{--}60$  min of operation, subsequently increasing slightly from  $6.14$  to  $6.63\text{ m}^{-1}$ ; and (iii) at the maximum filtration velocity of  $40\text{ m/h}$ , the  $X_L$  value is seen to decrease from  $7.14$  to  $6.31\text{ m}^{-1}$  during the initial  $10\text{--}60$  min of operation and subsequently remain stable within the range of  $6.02\text{--}6.31\text{ m}^{-1}$ . These results suggest that a low filtration velocity ( $20\text{ m/h}$ ) leads to gradual blockage of the pores in the media layer, and that uniform blockage occurs at  $30\text{ m/h}$ . This is probably a result of deep bed filtration behavior due to the removal of a larger fraction of SS in the sedimentation chamber and the introduction of a smaller fraction of SS into the filtration chamber, as described previously [20]. Moreover, the observation of a high  $X_L$  value at the beginning of operation at  $40\text{ m/h}$ , with a subsequent decrease over the operating time, also suggests that a substantial amount of SS is deposited during the initial period, with a smaller fraction being discharged thereafter.

Overall, an increase in the  $X_L$  value with increasing filtration velocity is observed during the initial  $10\text{--}60$  min of operation, thus suggesting an increased amount of blockage with increased inlet SS load [16,46]. Nevertheless, the present results indicate a convergence of the  $X_L$  towards similar values regardless of the filtration velocity as the operation period

is increased. Thus, the average and standard deviation of the  $X_L$  values at operating times of 180–300 min are  $6.31 \pm 0.27 \text{ m}^{-1}$  for the flowrate range of 20–40 m/h. This indicates that similar levels of SS deposition and blockage of the media layer are eventually reached (given sufficient operation time) regardless of filtration velocity.

In view of the above results, it was thought that the  $X_L$  parameter would be useful for investigating the blockage of the media layer. However, the tendency of the  $X_L$  value to vary with both operating time and filtration velocity might not readily allow a clear description of the SS removal. Therefore, the cumulative reduced SS load,  $X_\sigma$ , was calculated according to the specific SS deposit ( $\sigma$ ) (Equation (15)), and the results are presented in Figure 6C. Here,  $X_\sigma$  is seen to decrease almost linearly from 10.35 to  $-3.27 \text{ m}^{-1}$ , from 6.97 to  $-4.05 \text{ m}^{-1}$ , and from 6.23 to  $-4.97 \text{ m}^{-1}$ , at filtration velocities of 20, 30, and 40 m/h, respectively, during the period of operation. Moreover, the  $X_\sigma$  was well correlated with the natural logarithm of operation time ( $\ln(t)$ ) at each filtration velocity and with the filtration velocity at each operation time. These results indicate that the SS removal in the granular media layer can successfully be described by the steady-state porous media capture model based on the specific SS deposit.

### 3.3. Correlations between Head Loss and the Parameters $k_a$ , $k_d$ , $\sigma_m$ , and $X_\sigma$

The results described above indicate that the specific SS deposit ( $\sigma$ ) is useful for describing the SS removal for the media layer used in the present study (Figures 5E,F and 6C). Hence, various parameters related to the specific deposit, such as  $k_a$ ,  $k_d$ ,  $\sigma_m$ , and  $X_\sigma$ , can be correlated with the head loss, as shown in Figure 7. As reported previously, the total head loss in the media layer increases from 3.0 to 5.5 cm, from 4.2 to 6.5 cm, and from 5.6 to 7.9 cm, at flow velocities of 20, 30, and 40 m/h, respectively [20]. In the present work, the parameters  $k_a$ ,  $k_d$ , and the natural logarithm of  $\sigma_m$  exhibited good correlations with the final head loss (Figure 7A). In particular,  $k_a$  and the  $k_d$  are seen to increase, while  $\ln(\sigma_m)$  decreases as the final head loss increases. The increased  $k_a$  indicates that an enhanced SS deposit in the media layer leads to a decrease in the amount of pore space due to the SS accumulation therein. By contrast, the increased  $k_d$  indicates an increased possibility of re-dispersion with increased SS deposit ( $\sigma$ ) in the media layer [24,37]. This conclusion is supported by the observed decrease in  $\sigma_m$  with increasing head loss (i.e., with an increasing amount of SS deposit). In addition, the results in Figure 7B indicate that the final head loss decreases with increasing  $X_\sigma$ . As reported previously, both a higher head loss and a lower  $X_\sigma$  indicate a decreased SS permittivity and a more significant level of blockage [16]. Moreover, the previous studies report a linear correlation between the head loss and  $X_\sigma$  for  $X_\sigma$  values of  $<3$ , with fluctuations in the head loss at  $X_\sigma > 3$ , probably due to the re-dispersion of the deposited SS [38]. The present and previous results thus support the conclusion that an increased level of SS deposition is accompanied by an increased probability of re-dispersion.

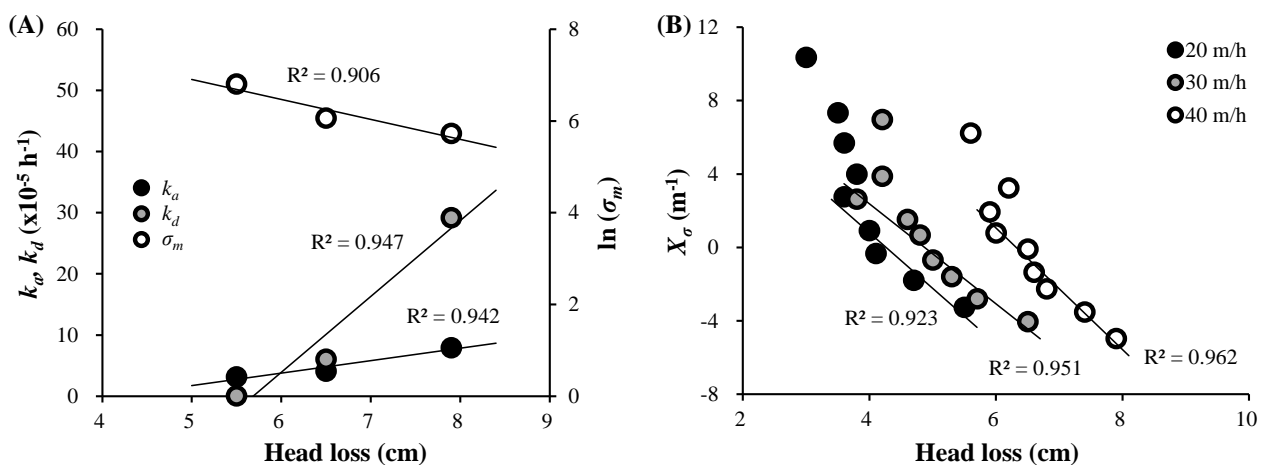


Figure 7. The correlations between the head loss and (A) the parameters  $k_a$ ,  $k_d$ , and  $\ln(\sigma_m)$ ; and (B)  $X_\sigma$ .

### 3.4. Applications

It is expected that the modeling approaches in this study would contribute to estimating the life of a media layer via the correlations of specific SS deposit ( $\sigma$ ) with filtration coefficient ( $X_\sigma$ ), the maximum specific SS deposit ( $\sigma_m$ ), and SS removal rate constant ( $X_\sigma$ ). The time variation of the SS in runoffs during a rainfall event was not considered, as mentioned above. However, the possibility of more improvement was confirmed by the successful description displayed in Figures 3, 5E and 6C, under irregular influent SS concentration.

In addition, the result of this study would also contribute to the further study by providing important information about the major consideration for the description and prediction of the performance of stormwater filtration systems, which are the dependence of  $k_a$ ,  $k_\sigma$ ,  $\sigma_m$ ,  $k_\sigma$ , and  $X_\sigma$  on filtration velocity, i.e., flowrate (Figures 3, 5E and 6C), and the dependence of  $k_a$ ,  $k_\sigma$ ,  $\sigma_m$ , and  $X_\sigma$  on head loss (Figure 7).

Moreover, the modeling approaches in this study would contribute to the evaluation of a stormwater filtration system in a laboratory. In many countries, a stormwater runoff treatment system is evaluated in a laboratory by relevant authorities before installation, because it is hard to monitor the performance on site [29,30,35,36]. The major information to be obtained are the life and critical specific SS deposit. However, they can hardly be obtained by the results of experiments performed in a short period. Therefore, a number of laboratory studies have been performed to evaluate the performance of stormwater runoff filtration systems [11,16,37,43–46].

## 4. Conclusions

In the present study, the performance of the granular media layer of an upflow stormwater filtration system was investigated using various models. The SS concentrations of the influent to, and effluent from, the media layer were found to fluctuate due to the irregular SS removal efficiency of the pretreatment (sedimentation) chamber.

A kinetic model, deep bed filtration model,  $k$ - $C^*$  model, and a porous media capture model under steady-state were investigated to describe SS removal in the media layer at various filtration velocities. The kinetic model was shown to provide a good fit for the time course of the specific deposit, while the parameters representing SS attachment, SS detachment, and maximum SS deposition were in good correlation with the filtration velocity. However, the deep bed filtration model did not provide a good correlation between the characteristic parameter (i.e., the filtration coefficient) and the specific deposit. The SS concentration and the SS load reduction were not well described by the  $k$ - $C^*$  model or the porous media capture model. However, modified versions of the  $k$ - $C^*$  model and the porous media capture model, in which a specific type of SS deposit was considered, were able to describe the system performance. It was possible to calculate the parameters characterizing the filtration behavior, and the results were in agreement with the measured SS removal. Moreover, the parameters of the kinetic model, the modified  $k$ - $C^*$  model, and the modified porous media capture model were each in good correlation with the specific deposit.

The results of this study suggest that models using a specific deposit can successfully describe the SS removal of granular media layers even when pretreated stormwater with a highly fluctuating SS concentration is introduced. However, it should be noted that a more improved model must be developed considering the time variation of the SS concentration in the stormwater runoff.

**Author Contributions:** Conceptualization, Y.H. and S.K.; methodology, D.K.; validation, Y.H. and D.K.; formal analysis, D.K.; investigation, Y.S.; resources, Y.H.; data curation, D.K.; writing—original draft preparation, Y.H. and Y.S.; writing—review and editing, D.K. and S.K.; visualization, D.K.; supervision, D.K.; project administration, Y.H.; funding acquisition, Y.H. All authors have read and agreed to the published version of the manuscript.

**Funding:** This research received no external funding.

**Institutional Review Board Statement:** Not applicable.

**Informed Consent Statement:** Not applicable.

**Data Availability Statement:** Not applicable.

**Acknowledgments:** This work was supported by the National Research Foundation of Korea (NRF) grant funded by the Korean Government (MSIT) (No. 2021R1F1A1064004). We acknowledge C & C Inc. (Republic of Korea) for supplying the granular media used in this study.

**Conflicts of Interest:** The authors declare no conflict of interest.

## References

1. USEPA. Polluted Runoff: Nonpoint Source (NPS) Pollution. Available online: <https://www.epa.gov/nps> (accessed on 1 April 2021).
2. Xin, X.; Yin, W.; Li, K. Estimation of non-point source pollution loads with flux method in Danjiangkou Reservoir area, China. *Water Sci. Eng.* **2017**, *10*, 134–142. [[CrossRef](#)]
3. Korea Office of Prime Minister, Ministry for Food, Agriculture, Forestry and Fisheries, Korea Ministry of Knowledge Economy, Korea Ministry of Environment, Korea Ministry of Infrastructure and Transport, Korea Nation fire Agency, Korea Rural Development Administration, Korea Forest Service. The third comprehensive non-point sources management plan (2021–2025). 2020. (In Korean)
4. Kim, D.G.; Ko, S.O. Road-deposited sediments mediating the transfer of anthropogenic organic matter to stormwater runoff. *Environ. Geochem. Health* **2020**. [[CrossRef](#)] [[PubMed](#)]
5. Chen, H.; Liao, Z.; Gu, X.; Xie, J.; Li, H.; Zhang, J. Anthropogenic influences of paved runoff and sanitary sewage on the dissolved organic matter quality of wet weather overflows: An excitation?emission matrix parallel factor analysis assessment. *Environ. Sci. Technol.* **2017**, *51*, 1157–1167. [[CrossRef](#)] [[PubMed](#)]
6. Hosen, J.D.; McDonough, O.T.; Febria, C.M.; Palmer, M.A. Dissolved organic matter quality and bioavailability changes across an urbanization gradient in headwater streams. *Environ. Sci. Technol.* **2014**, *48*, 7817–7824. [[CrossRef](#)]
7. Wang, Q.; Zhang, Q.; Dzakpasu, M.; Chang, N.; Wang, X. Transferral of HMs pollution from road-deposited sediments to stormwater runoff during transport processes. *Front. Environ. Sci. Eng.* **2019**, *13*, 13. [[CrossRef](#)]
8. Borris, M.; Österlund, H.; Marsalek, J.; Viklander, M. Contribution of coarse particles from road surfaces to dissolved and particle-bound heavy metal loads in runoff: A laboratory leaching study with synthetic stormwater. *Sci. Total Environ.* **2016**, *573*, 212–221. [[CrossRef](#)] [[PubMed](#)]
9. Yang, Y.-Y.; Toor, G.S. Stormwater runoff driven phosphorus transport in an urban residential catchment: Implications for protecting water quality in urban watersheds. *Sci. Rep.* **2018**, *8*, 11681. [[CrossRef](#)]
10. Ahn, J.; Lee, D.; Han, S.; Han, A.; Jung, Y.; Park, S.; Choi, H. Experimental study on performance of sand filter layer to remove non-point source pollutants in rainwater. *Water Sci. Technol.* **2017**, *17*, 1748–1763. [[CrossRef](#)]
11. Siriwardene, N.R.; Deletic, A.; Fletcher, T.D. Clogging of stormwater gravel infiltration systems and filters: Insights from a laboratory study. *Water Res.* **2007**, *41*, 1433–1440. [[CrossRef](#)]
12. Gironás, J.; Adriasola, J.M.; Fernández, B. Experimental analysis and modeling of a storm water perlite filter. *Water Environ. Res.* **2008**, *80*, 524–539. [[CrossRef](#)]
13. Hsieh, C.; Davis, A.P. Evaluation and optimization of bioretention media for treatment of urban storm water runoff. *J. Environ. Eng. ASCE* **2005**, *131*, 1521–1531. [[CrossRef](#)]
14. Hoslett, J.; Massara, T.M.; Malamis, S.; Ahmad, D.; van den Boogaert, I.; Katsou, E.; Ahmad, B.; Ghazal, H.; Simons, S.; Wrobel, L.; et al. Surface water filtration using granular media and membranes: A review. *Sci. Total Environ.* **2018**, *639*, 1268–1282. [[CrossRef](#)]
15. Lim, H.S.; Lim, W.; Hu, J.Y.; Ziegler, A.; Ong, S.L. Comparison of filter media materials for heavy metal removal from urban stormwater runoff using biofiltration systems. *J. Environ. Manag.* **2015**, *147*, 24–33. [[CrossRef](#)]
16. Franks, C.A.; Davis, A.P.; Aydilek, A.H. Geosynthetic filters for water quality improvement of urban storm water runoff. *J. Environ. Eng. ASCE* **2012**, *138*, 1018–1028. [[CrossRef](#)]
17. Shan, G.; Surampalli, R.Y.; Tyagi, R.D.; Zhang, T.C. Nanomaterials for environmental burden reduction, waste treatment, and non-point source pollution control: A review. *Front. Environ. Sci. Eng.* **2009**, *3*, 249–264. [[CrossRef](#)]
18. Cheng, J.; Yuan, Q.; Kim, Y. Long-term operational studies of lab-scale pumice-woodchip packed stormwater biofilters. *Environ. Technol.* **2018**, *39*, 1765–1775. [[CrossRef](#)] [[PubMed](#)]
19. Yi, S.-J.; Kim, Y.-I. Improvement on management of non-point source pollution for reasonable implementation of TMDL—Focusing on selection of non-point source pollution management region and management of non-point source pollutant. *J. Korean Soc. Environ. Eng.* **2014**, *36*, 719–723. [[CrossRef](#)]
20. Hwang, Y.; Seo, Y.; Kim, H.; Roh, K.; Shin, H.; Kim, D. Optimization of Operation and Backwashing Condition for an Upflow Stormwater Filtration System Utilizing Ceramic Media. *J. Korean Soc. Environ. Eng.* **2017**, *39*, 478–488. (In Korean) [[CrossRef](#)]
21. Boller, M.A.; Kavanaugh, M.C. Particle characteristics and headloss increase in granular media filtration. *Water Res.* **1995**, *29*, 1139–1149. [[CrossRef](#)]
22. Rodgers, M.; Mulqueen, J.; Healy, M.G. Surface Clogging in an Intermittent Stratified Sand Filter. *Soil Sci. Soc. Am. J.* **2004**, *68*, 1827–1832. [[CrossRef](#)]

23. Kang, S.; Kim, S.; Lee, S.; Lee, T. An upflow-type filtration device using expanded polypropylene media (EPM) to treat first flush of rainwater. *Water Environ. Res.* **2016**, *88*, 195–200. [[CrossRef](#)]
24. Lee, J.J.; Johir, M.A.H.; Chinu, K.H.; Shon, H.K.; Vigneswaran, S.; Kandasamy, J.; Kim, C.W.; Shaw, K. Novel pretreatment method for seawater reverse osmosis: Fibre media filtration. *Desalination* **2009**, *250*, 557–561. [[CrossRef](#)]
25. Zhang, W.; Sang, M.; Che, W.; Sun, H. Nutrient removal from urban stormwater runoff by an up-flow and mixed-flow bioretention system. *Environ. Sci. Pollut. Res.* **2019**, *26*, 17731–17739. [[CrossRef](#)] [[PubMed](#)]
26. Lee, J.; Lee, M. Stormwater runoff treatment filtration system and backwashing system. *Water Sci. Technol.* **2019**, *79*, 771–778. [[CrossRef](#)]
27. Marsalek, J.; Jimenez-Cisneros, B.E.; Karamouz, M.; Malmquist, P.-A.; Goldenfum, J.; Chocat, B. *Urban Water Cycle Processes and Interactions*; CRC Press: Boca Raton, FL, USA, 2008.
28. Rügner, H.; Schwientek, M.; Milačić, R.; Zuliani, T.; Vidmar, J.; Paunović, M.; Laschou, S.; Kalogianni, E.; Skoulikidis, N.T.; Diamantini, E.; et al. Particle bound pollutants in rivers: Results from suspended sediment sampling in Globaqua River Basins. *Sci. Total Environ.* **2019**, *647*, 645–652. [[CrossRef](#)]
29. British Water. *Code of Practice—Assessment of Manufactured Treatment Devices Designed to Treat Surface Water Runoff*; British Water: London, UK, 2017.
30. Auckland Regional Council. *Proprietary Devices Evaluation Protocol (PDEP) for Stormwater Quality Treatment Devices, Version 3*; Auckland Regional Council: Auckland, New Zealand, 2012.
31. Yun, Y.; Park, H.; Kim, L.; Ko, S. Size Distributions and Settling Velocities of Suspended Particles from Road and Highway. *KSCE J. Civ. Eng.* **2010**, *14*, 481–488. [[CrossRef](#)]
32. Cho, Y.-J.; Lee, J.-H.; Bang, K.-W.; Cho, S.C.-S. Water Quality and Particle Size Distributions of Bridge Road Runoff in Storm Event. *J. Korean Soc. Environ. Eng.* **2007**, *29*, 1353–1359. (In Korean)
33. Lee, H.; Lee, S. Runoff Characteristics of Stormwater in Small City Urban Area. *J. Korean Soc. Environ. Eng.* **2009**, *31*, 193–202. (In Korean)
34. APHA; AWWA; WEF. *Standard Methods for the Examination of Water and Wastewater*, 22nd ed.; APHA: Washington, DC, USA, 2012.
35. Korea Ministry of Environment. *Installation and Operation Manual of Non-Point Pollution Reduction Facility*; Korea Ministry of Environment: Sejong-si, Korea, 2020.
36. New Jersey Department of Environmental Protection (NJDEP). *New Jersey Department of Environmental Protection Laboratory Protocol to Assess Total Suspended Solids Removal by a Filtration Manufactured Treatment Device*; New Jersey Department of Environmental Protection: Trenton, NJ, USA, 2013.
37. Sikorska, E.; Gac, J.M.; Gradoń, L. Performance of a depth fibrous filter at particulate loading conditions: Description of temporary and local phenomena with structure development. *Chem. Eng. Res. Des.* **2018**, *132*, 743–750. [[CrossRef](#)]
38. Przekop, R.; Gradoń, L. Dynamics of particle loading in deep-bed filter: Transport, deposition and re entrainment. *Chem. Process Eng.* **2016**, *37*, 405–417. [[CrossRef](#)]
39. Nakamura, K.; Nakamura, J.; Matsumoto, K. Filtration and backwashing behaviors of the deep bed filtration using long length poly-propylene fiber filter media. *J. Taiwan. Inst. Chem. Eng.* **2019**, *94*, 31–36. [[CrossRef](#)]
40. Santos, A.; Barros, P.H.L. Multiple Particle Retention Mechanisms during Filtration in Porous Media. *Environ. Sci. Technol.* **2010**, *44*, 2515–2521. [[CrossRef](#)] [[PubMed](#)]
41. Santos, A.; Araújo, J.A. Modeling Deep Bed Filtration Considering Limited Particle Retention. *Transp. Porous Med.* **2015**, *108*, 697–712. [[CrossRef](#)]
42. Bai, R.; Tien, C.A. A new correlation for the initial filter coefficient under unfavorable surface interactions. *J. Colloid Interf. Sci.* **1996**, *179*, 631–634. [[CrossRef](#)]
43. Kadlec, R.H.; Knight, R.L. *Treatment Wetlands*; CRC Press: Boca Raton, FL, USA, 1996.
44. Wong, T.H.F.; Fletcher, T.D.; Duncan, H.P.; Jenkins, G.A. Modelling urban stormwater treatment-A unified approach. *Ecol. Eng.* **2006**, *27*, 58–70. [[CrossRef](#)]
45. Siriwardene, N.R.; Deletic, A.; Fletcher, T.D. Modeling of Sediment Transport through Stormwater Gravel Filters over Their Lifespan. *Environ. Sci. Technol.* **2007**, *41*, 8099–8103. [[CrossRef](#)] [[PubMed](#)]
46. American Water Works Association (AWWA). *Water Quality and Treatment*, 5th ed.; McGraw-Hill: New York, NY, USA, 1999.
47. Campos, L.C. Modelling and Simulation of the Biological and Physical Processes of Slow Sand Filtration. Ph.D. Thesis, Imperial College of Science Technology and Medicine, London, UK, 2002.
48. Wakeman, R. The influence of particle properties on filtration. *Sep. Purif. Technol.* **2007**, *58*, 234–241. [[CrossRef](#)]
49. Newton, D. The Effectiveness of Modular Porous Pavement as a Stormwater Treatment Device. Ph.D. Thesis, Griffith University, Brisbane, Australia, 2005.
50. Qin, H.; He, K.; Fu, G. Modeling middle and final flush effects of urban runoff pollution in an urbanizing catchment. *J. Hydrol.* **2016**, *534*, 638–647. [[CrossRef](#)]
51. Alam, M.Z.; Anwar, A.H.M.F.; Heitz, A. Stormwater solids removal characteristics of a catch basin insert using geotextile. *Sci. Total Environ.* **2018**, *618*, 1054–1063. [[CrossRef](#)]